THE JOURNAL OF BIOLOGICAL CHEMISTRY VOL. 287, NO. 18, pp. 14703–14717, April 27, 2012

Disruption of Proprotein Convertase 1/3 (PC1/3) Expression in Mice Causes Innate Immune Defects and Uncontrolled Cytokine Secretion*[S]

Received for publication, November 14, 2011, and in revised form, February 14, 2012 Published, JBC Papers in Press, March 6, 2012, DOI 10.1074/jbc.M111.323220

Sarah Refaie[‡1], Sandra Gagnon[‡1], Hugo Gagnon[‡§], Roxane Desjardins[‡], François D'Anjou[‡], Pedro D'Orléans-Juste[‡], Xiaorong Zhu[¶], Donald F. Steiner[¶], Nabil G. Seidah[‖], Claude Lazure[‖], Michel Salzet[§], and Robert Day[‡2]

From the [‡]Institut de pharmacologie de Sherbrooke, Université de Sherbrooke, Sherbrooke, Québec J1H 5N4, Canada, [¶]Department of Medicine, University of Chicago, Chicago, Illinois 60637, [‖]Institut de Recherches Cliniques de Montréal (IRCM), Montreal, Quebec H2W 1R7, Canada, and [§]Université Lille Nord de France, Laboratoire de Spectrométrie de Masse Biologique Fondamentale et Appliquée-EA4550, Université Lille 1, IFR 147, bâtiment SN3, 59655 Villeneuve d'Ascq, France

Background: PC1/3 is known for its role in neuroendocrine cells but not for its potential role in innate immunity.
Results: PC1/3 knock-out mice express a dysfunctional phenotype characterized by uncontrolled cytokine secretion when challenged with lipopolysaccharide.
Conclusion: PC1/3 regulates cytokine secretion in macrophages.
Significance: Identifying the role of PC1/3 in macrophages will lead to a better understanding of cytokine regulation and innate immunity.

The proprotein convertase 1/3 is expressed in the regulated secretory pathway of neural and endocrine cells. Its major function is in the post-translational processing and activation of precursor proteins. The PC1/3 knock-out (KO) mouse model has allowed us to elucidate its physiological functions in studies focused primarily on neuroendocrine tissues. However, PC1/3 is also expressed in cells of the immune system, mainly in macrophages. The present study explores the effects of innate immune challenge in the PC1/3 KO mouse. PC1/3 KO mice have an enlarged spleen with marked disorganization of the marginal zone and red pulp. Immunohistochemical studies using various markers demonstrate a depletion of dendritic cells in PC1/3 KO spleens. When challenged with lipopolysaccharide, PC1/3 KO mice are more susceptible to septic shock than wild-type controls or other PC KO mice, such as PC2 and PC7 null mice. Plasma levels of proinflammatory cytokines (IL-6, IL-1β, and TNF-α) were very significantly elevated in PC1/3 KO mice, consistent with a hypercytokinemia, *i.e.* indicative of a major systemic uncontrolled inflammatory response or cytokine storm. Peritoneal macrophages isolated from PC1/3 KO mice also demonstrate elevated cytokine secretion when treated with LPS. Electron micrographs show morphological features indicating a prolonged activation of these cells following LPS stimulation. We also present evidence that the proinflammatory T_h1 pathway is dominant in the PC1/3 KO mouse model. We conclude that aside from its important role in neuroendocrine functions PC1/3 also has an important role in the regulation of the innate immune system, most likely through the regulation of cytokine secretion in macrophages.

Proprotein convertases (PCs)[3] are a family of enzymes whose main function is the first step of an enzymatic cascade that includes the endoproteolytic cleavage of inactive precursor proteins and the subsequent processing into bioactive proteins and peptides by carboxypeptidases and amidating enzymes (1, 2). The PCs form a family of subtilisin-like serine proteinases encoded by nine genes, *PCSK1* to *PCSK9* (PC subtilisin/kexin), coding for PC1/3, PC2, furin, PC4, PC5/6, PACE4, PC7, SKI-1/S1P, and PCSK9, respectively (3–7). Seven PCs cleave secretory precursors at single or paired basic amino acids within a recognized cleavage site, R*X*(R/K)R ↓ (3), whereas SKI-1/S1P does not require a basic amino acid at the cleavage site. As for PCSK9, it functions only as a binding protein targeting for degradation in lysosomes among others the low density lipoprotein receptor. PC cleavages result in a diversity of bioactive products, zymogen activation, and sometimes inactivation of key proteins (4).

Some PCs are expressed ubiquitously in the organism, such as furin (8, 9), or are widespread like PC5/6 and PC7, whereas others are more organ- or system-specific (10). For example, PC1/3 has been associated with the neuroendocrine system where its expression was first reported (11–13). However, a few studies have identified an atypical expression of PC1/3 in cells of the immune system; namely PC1/3 has been detected in a human monocyte-derived macrophage cell line (14), differentiated macrophages (15), and immune organs, such as the spleen, thymus, and lymphatic ganglia (16).

* This work was supported in part by the Canadian Institutes of Health Research.
[S] This article contains supplemental Figs. 1–5.
[1] These authors contributed equally to this work.
[2] A member of the Centre de Recherche Clinique Etienne-Le Bel (Sherbrooke, Québec, Canada). To whom correspondence should be addressed: Inst. de pharmacologie de Sherbrooke (IPS), Faculté de Médecine et des Sciences de la Santé (FMSS), Université de Sherbrooke, 3001 12e Ave. Nord, Sherbrooke, Québec J1H 5N4, Canada. Tel.: 819-564-5428; Fax: 819-820-6886; E-mail: Robert.day@usherbrooke.ca.

[3] The abbreviations used are: PC, proprotein convertase; PCSK, PC subtilisin/kexin; TLR, Toll-like receptor; T_h, T helper; TEM, transmission electron microscopy; APC, antigen-presenting cell; DC, dendritic cell; LD_{100}, lethal dose; MAP, mean arterial blood pressure; EDV, electron-dense vesicle.

In a previous study, we showed that both neuroendocrine-"specific" convertases, namely PC2 and PC1/3, are also expressed in macrophages and lymphocytes *in vivo* (16) and are highly responsive to pathogen-associated molecular pattern challenge. We also showed a coordinated induction of proenkephalin (a PC1/3 and PC2 substrate), PC1/3, and PC2 mRNAs as well as proenkephalin-derived peptides (*i.e.* enkelytin) in macrophage subpopulations (17, 18). Although these data support the notion of a neuroendocrine phenotypic plasticity in immune cells (19), they show that the expression of PC2 and PC1/3 is regulated by challenges (*e.g.* pathogen-associated molecular patterns) that activate the innate immune system, suggesting a role in innate immunity. Macrophages are crucial in the innate immune system, and their activation is mediated via recognition of various pathogen-associated molecular patterns by specific toll-like receptors (TLRs) (20). TLR4, for example, binds and recognizes lipopolysaccharides (LPSs) to initiate an immune reaction, including cytokine secretion (21, 22). Communication with the acquired immune system is also essential to control the immune response. This is commonly accomplished by activating and recruiting T helper (T_h) cells that can differentiate into T_h1 or T_h2 cells to further activate or attenuate, respectively, the immune response (23, 24). Specific cytokine profiles are observed for the T_h1 cytotoxic pathway, such as IL-12 and IFN-γ (25, 26), and the T_h2 humoral pathway in which IL-10, IL-4, and IL-5 are secreted (27).

We also noted previously that PC1/3 expression in the spleen (16) was mostly confined to the red pulp regions known to be rich in macrophages (28) and was increased after LPS stimulation. Co-localization of PC1/3 with CD14, a macrophage marker (29), sparked our interest in investigating the role of PC1/3 in macrophages to elucidate the function of PC1/3 in the innate immune system. Disruption of the gene encoding PC1/3 has revealed a phenotype associated with postnatal growth impairment and multiple defects in the processing of neuroendocrine peptide precursors, including hypothalamic growth hormone-releasing hormone, pituitary proopiomelanocortin to adrenocorticotropic hormone, islet proinsulin to insulin, and intestinal proglucagon to glucagon-like peptide-1 and -2 (30–34). However, in the present study, we hypothesized that an immune phenotype might become more evident in PC1/3 KO mice if they were submitted to a challenge, such as with LPS, which triggers a cascade of events subsequent to the stimulation of TLR4 receptors. Indeed, we uncovered a massive cytokine response, which is highly lethal due to a lack of regulation of cytokine secretion *in vivo*. We also demonstrate that the T_h1 pathway, indicative of a proinflammatory response, is enhanced in PC1/3 KO mice. Our data thus suggest that PC1/3 plays a vital role in the secretory response of macrophages to pathogen challenge.

EXPERIMENTAL PROCEDURES

Mouse Experimental Models—Transgenic PC1/3, PC2, and PC7 KO mice as well as wild-type (WT) mice used in this study were between 3 and 6 months of age. The mice were held in a pathogen-free environment and were given food and water *ad libitum*. PC1/3 KO and PC2 KO mice have been described (30). PC1/3 KO mice were generated by the deletion of exon 1 and several upstream transcriptional control elements of the *PCSK1* gene by inserting a neomycin cassette in the C57Bl/6 mouse background as described previously (30). PC2 KO mice have a mutation in the third exon of the *PCSK2* gene that leads to the synthesis of a defective enzyme that is subsequently degraded (35). PC7 KO mice were generated by deleting exons 3–7 of the *PCSK7* gene, which yields a protein containing an inactive catalytic site (36). PC1/3, PC2, and PC7 KO mouse backgrounds were changed from C57Bl/6 to CD1 with over 20 backcrosses each. All experimental procedures were in accordance with the Canadian Council on Animal Care.

Spleen Characterization and Immunohistochemical Staining—WT and PC1/3 KO mice were euthanized by cervical dislocation. Spleens were extracted and weighed. Standard preparation procedures of paraffin-embedded tissues and H&E stain were used. Immunostaining was done with the Dako Autostainer Plus (Dako, Burlington, Ontario, Canada) using primary antibodies directed against CD3, CD4, CD7, CD15, CD20, CD21, CD22, CD56, CD57, CD68, and IgM (Dako) according to the manufacturer's instructions. A secondary antibody coupled to HRP (Dako) was then applied followed by a Harris hematoxylin counterstain according to the manufacturer's specifications. Immunostained spleens were examined using the Axioskop 2 phase-contrast microscope (Carl Zeiss, Inc., Thornwood, NY). Photomicrographs of 1392 × 1040 pixels were captured using a 10× or 40× objective and a Retiga SRV cooled color digital camera (QImaging, Burnaby, British Columbia, Canada). The images were processed using Image Pro software (Media Cybernetics, Silver Springs, MD).

Endotoxin Shock and Determination of Plasma Cytokine Content following LPS in Vivo Challenge—Mice were injected with *Escherichia coli* 0127:B8 lipopolysaccharide (LPS) (Sigma-Aldrich) at a lethal dose (LD_{100}) of 25 mg/kg (intraperitoneally). Mice were monitored for a 3-day period to observe survival rates. Time course experiments were also performed by injecting 100 μg of LPS intraperitoneally into mice for 0, 4, 8, and 24 h. For plasma cytokine content, blood was collected by cardiac puncture, and plasma was isolated by centrifugation. Cytokines were measured using an ELISA kit (R&D Systems, Minneapolis, MN) specific for mouse IL-6, TNF-α, IL-1β, IL-12p70, IL-10, and IFN-γ. Statistical analysis was performed by applying the *t* test parameters (Prism 5, GraphPad Software, La Jolla, CA).

Determination of Cytokine Secretion and Cellular Content of Primary Peritoneal Macrophages—Mice were injected intraperitoneally with 2 ml of sterile 3% thioglycolate (BD Biosciences) to increase the yield of peritoneal macrophages. Three days later, mice were anesthetized with ketamine/xylazine (87/13 mg/kg intramuscularly) and then sacrificed by cervical dislocation. Peritoneal cells were collected by peritoneal wash with a phosphate-buffered saline (PBS) solution. Red blood cells were lysed by incubating the cells with hemolysis buffer. Cells were plated in a 6- or 24-well plate at 8×10^5 or 2.4×10^6 cells, respectively, for 24 h at 37 °C in a humidified atmosphere of 5% CO_2 in air to allow macrophage adherence, which purifies the peritoneal exudates. The cell medium consisted of RPMI 1640 medium and penicillin/streptomycin. The following day, the medium was changed, and cells were stimulated with 1×

PBS or 100 ng/ml LPS without serum for 4 h. Medium was collected, and cell lysate was obtained by adding 200 μl of 0.5 N HCl followed by three freeze-thaw cycles. Protein contents were collected by centrifugation, and cytokines were measured using ELISA kits specific for mouse IL-6, TNF-α, and IL-1β according to the manufacturer's instructions (R&D Systems). Statistical analysis was done using a Student's *t* test algorithm in Prism 5 (GraphPad Software), which calculated the S.E.

Measurement of Arterial Blood Pressure in Mice—Mice were anesthetized with ketamine/xylazine (87/13 mg/kg intramuscularly). A polyethylene catheter (PE-10) containing a heparin/saline solution was inserted into the common right carotid artery to monitor the arterial blood pressure via a transducer linked to a polygraph (Grass Instrument Co., Baintree, MA). Another catheter (PE-10) was inserted into the left jugular vein to inject LPS at a dose of 2.2 mg/kg.

RNA Extraction, Reverse Transcription, Quantitative PCR, and PC1/3 Sequencing—The RNA of peritoneal macrophages and tissues was extracted with TRIzol (Invitrogen) reagent and chloroform. The reverse transcription and quantitative PCR procedure was described previously (37). ProSAAS primers were described previously (38). For PC1/3 cDNA sequencing, the same procedure was used except that the PCR was done with 1 unit of *Taq* DNA polymerase (Roche Diagnostics). The resulting cDNA was next cloned in pGEM-T-Easy vector (Promega, Madison, WI) according to the manufacturer's instructions for sequencing. The sequences of the primers used for the PCR were as follows: mIL-6: forward, 5′-ACA AGT CGG AGG CTT AAT TAC ACA T-3′; reverse, 5′-AAT CAG AAT TGC CAT TGC ACA A-3′; mIL-1β: forward, 5′-GAG AAT GAC CTG TTC TTT GAA GTT GA-3′; reverse, 5′-TGA AGC TGG ATG CTC TCA TCT G-3′; mTNF-α: forward, 5′-CGT GGA ACT GGC AGA AGA G-3′; reverse, 5′-ACA AGC AGG AAT GAG AAG AGG-3′; mPC1/3: 91 bp forward, 5′-ATT TTG GTG CTG CTG CTC TT-3′; 91 bp reverse, 5′-GGA GTG CTC GTC TCA ACC A-3′; 252 bp forward, 5′-AGC AAA GAG GTT GGA CTC TGC-3′; 252 bp reverse, 5′-TAT GAA GAG CGC TTC TTC GGG-3′; and mActin: forward, 5′-GGG AAA TCG TGC GTG ACA TCA AAG-3′; reverse, 5′-CAT ACC CAA GAA GGA AGG CTG GAA-3′.

Transmission Electron Microscopy (TEM) of Peritoneal Macrophages—Peritoneal macrophages were collected as described above and directly subjected to a TEM procedure described previously (39). All images were taken at 60 kV and 3000× direct magnification. Images were analyzed with ImageJ software. Four different observers, among which three counted the images blindly, analyzed all structural features. An equal variance bilateral Student's *t* test was performed for statistical analysis.

Western Blotting of PC1/3—Pituitary glands from WT and KO mice were collected and disrupted in radioimmune precipitation assay lysis buffer containing Complete Mini protease inhibitor (Roche Diagnostics). Mouse peritoneal macrophages were collected and cultured at 4×10^7 cells as described above. The cells were lysed with 500 μl of radioimmune precipitation assay lysis buffer containing Complete Mini protease inhibitor. Equal amounts of protein were subjected to 8.5% SDS-PAGE and transferred to nitrocellulose (Amersham Biosciences Hybond ECL, GE Healthcare). The antibody directed against the C terminus of PC1/3 (9212) was described previously (40). PC1/3 was revealed by a goat anti-rabbit IgG coupled to IRDye 800 (LI-COR Biosciences, Lincoln, NE) with an infrared LI-COR Odyssey Imager (LI-COR Biosciences).

Gel LC-MS/MS Identification of PC1/3—Membrane protein fraction of macrophages was prepared as described previously (41). Briefly, cells were lysed and centrifuged at 16,000 × *g* to pellet membrane proteins. Proteins were solubilized and recovered by standard acetone/methanol precipitation. 20 μg of reconstituted protein were next separated on a precast 4–12% gradient acrylamide gel using freshly made MES buffer according to the manufacturer's protocol. The gel was stained with an MS-compatible silver stain (Invitrogen). The entire gel lane was excised into 18 bands, and each band was cut in 1-mm^3 pieces. The in-gel digestion protocol is based on the results obtained by Havlis *et al.* (42). Briefly, gel pieces were destained, proteins were reduced (10 mM DTT, 100 mM ammonium bicarbonate) and alkylated (55 mM iodoacetamide, 100 mM ammonium bicarbonate), and finally digested with 6 ng/ml sequencing grade trypsin (Promega). The resulting tryptic peptides were purified and identified by reverse phase LC coupled to an LTQ-Orbitrap (ThermoElectron). Protein identification was done with Scaffold V3.1.2 (Proteome Software Inc., Portland, OR) to validate MS/MS-based peptide and protein identifications from Mascot V2.1 (Matrix Science, London, UK) and X! Tandem version 2007.01.01.1 (The Global Proteome Machine).

RESULTS

Splenic Abnormalities in PC1/3 KO Mice—Splenomegaly was observed in the PC1/3 KO mice as shown in Fig. 1 (*A* and *B*) that was evident by comparing the weight of the spleens (~1.8-fold increase). An H&E stain was performed on cross-sections of the spleen to visualize its organizational structure. The staining allows the distinction of red and white pulp of the spleen. In PC1/3 KO spleens, the white pulp was more concentrated in the middle of the spleen with apparent fusion of white pulp nodes; this was not observed in WT mice. Some white pulp nodes were observed forming in the periphery of the PC1/3 KO spleen. The marginal zone, an important area of communication between macrophages and T cells (43, 44), shows an abnormal structure and blends with the red pulp in PC1/3 KO mice (Fig. 1, *D*–*G*). This spleen disorganization is also characterized by an increased presence of lymphocytes, represented as small *blue* cells, in the red pulp of PC1/3 KO spleen. Because the spleen is an important immune organ that monitors the circulating blood for infections, especially polysaccharide-encapsulated bacteria (45), and it requires the proper function of antigen-presenting cells (APCs), such as macrophages, dendritic cells (DCs), and B cells. We also conducted an RT-PCR experiment to confirm PC1/3 expression in spleen as well as expression of its known binding protein, proSAAS (Fig. 1*C*). The observation of a structural disorganization in the PC1/3 KO spleen led us to further investigate the role of PC1/3 in the innate immunity using LPS challenge.

PC1/3 KO Mice Are More Susceptible to Septic Shock Provoked by LPS—Septic shock is induced by an exaggerated immune response to an infection characterized by an uncon-

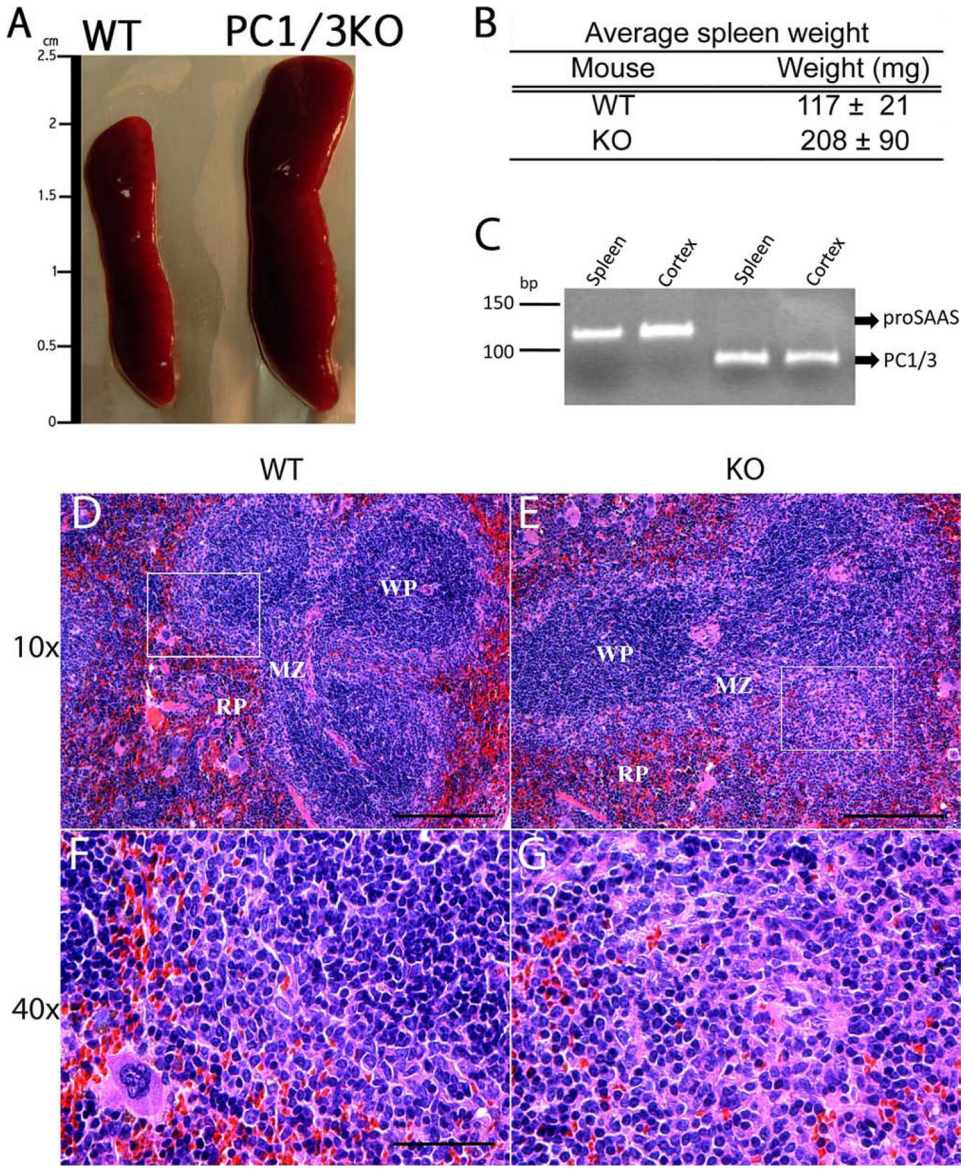

FIGURE 1. **WT and PC1/3 KO mouse spleen characterization and comparison.** *A*, relative size of PC1/3 KO (*right*) mouse spleen compared with WT (*left*). *B*, average weights of spleens from WT and PC1/3 KO mice. Data represent mean ± S.D. (p value <0.05; $n = 7$). *C*, RT-PCR product was obtained using RNA extract from WT mouse spleen and cortex (positive control) and then electrophoresed on a 10% acrylamide gel stained with ethidium bromide. 119- and 91-bp fragments were observed, correlating with the expected lengths for proSAAS and PC1/3, respectively. *D–G*, hematoxylin and eosin staining of cross-sections of WT (*D* and *F*) and PC1/3 KO (*E* and *G*) mouse spleens. A magnification at 40× (*E* and *F*) represents the framed region shown in the 10× magnification (*C* and *D*) of the respective spleen. Spleen regions are indicated, including the red pulp (*RP*), white pulp (*WP*), and marginal zone (*MZ*).

trolled secretion of proinflammatory cytokines. During Gram-negative bacterial infection, in most cases the initiator of this response is LPS, which is first recognized by innate immune mediators (*i.e.* macrophages) via the TLR4 (46). To study the role of PC1/3 in the innate immune system, a sepsis model was used to examine the survival rates of PC1/3 KO mice under endotoxemic conditions. The model consisted of injecting an LD_{100} of LPS and monitoring the survival rates for 3 days. In the case of WT mice, 50% of the mice were deceased between 24 and 30 h following LPS treatment, and most WT mice did not survive after 72 h (Fig. 2*A*). In contrast, all the PC1/3 KO mice were deceased 24 h post-LPS treatment (Fig. 2*A*).

To verify whether this phenotype was shared among other PCs, we carried out a similar analysis using available PC2 and PC7 null mice. We observed similar patterns of survival rates in PC2 and PC7 KO mice compared with their associated WT mice in this sepsis model (Fig. 2, *B* and *C*). These results indicate that PC1/3 KO mice are more susceptible to septic shock when administered a lethal dose of LPS as compared with WT or even other PC null mouse models. Therefore, PC1/3 seems to provide an important protective role during LPS-induced sepsis.

Effect of LPS Stimulation on Plasma Cytokine Concentrations over Time—Septic shock is primarily characterized by an unbalanced secretion of proinflammatory cytokines causing different symptoms associated with the pathology, such as systemic fever and inducible nitric-oxide synthase-dependent vasodilatation (47), resulting in a marked hypotensive response *in vivo* (48). To verify the effects of LPS on blood pressure in our mouse models, we measured and compared the mean arterial blood pressure (MAP) following LPS stimulation for a period of

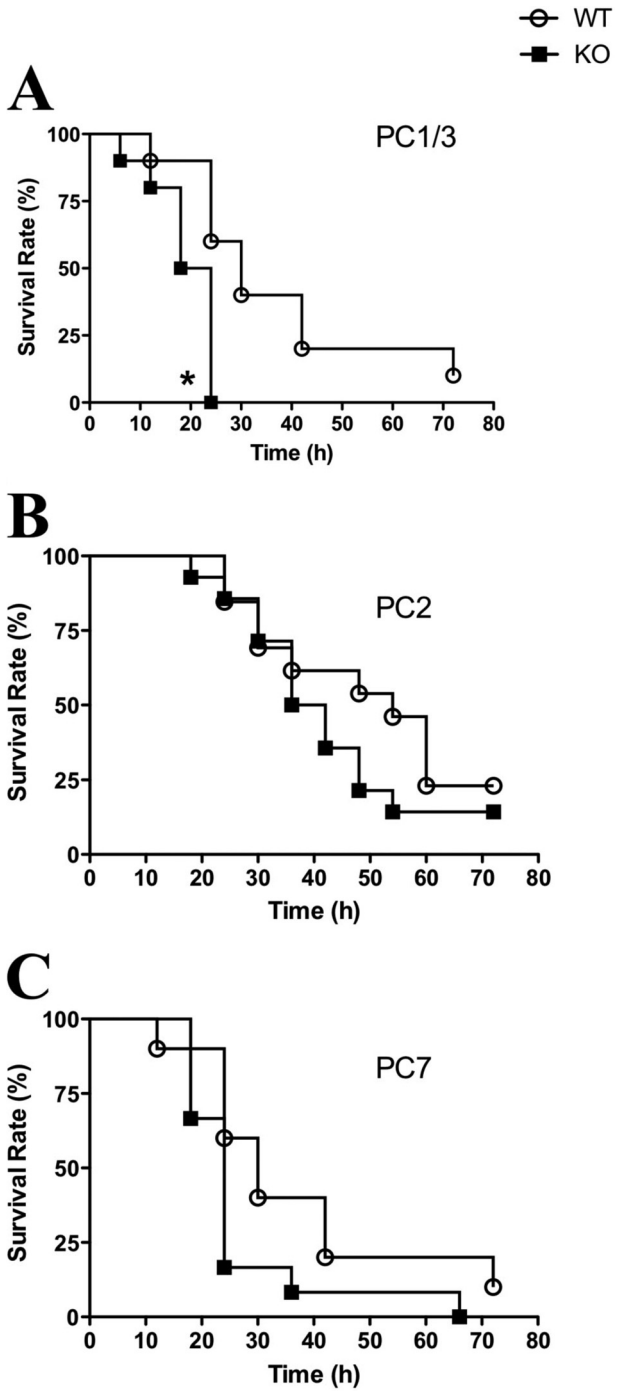

FIGURE 2. **Kaplan-Meier survival rates of mice challenged with LPS stimulation.** Survival curves of PC1/3 KO (*A*), PC2 KO (*B*), and PC7 KO (*C*) mice compared with the respective WT mice injected intraperitoneally with a lethal dose of LPS (25 mg/kg). Data represent mean ± S.E. (n = 10–14; *, $p < 0.05$).

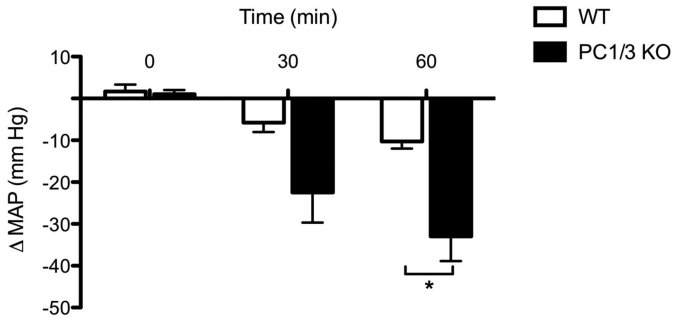

FIGURE 3. **MAP measured in mice following LPS stimulation.** MAP was observed in WT and PC1/3 KO mice followed by intravenous injection of 2.2 mg/kg LPS. MAP was measured for a period of 60 min after LPS stimulation. Data represent mean ± S.E. (n = 3–5; *, $p < 0.05$).

60 min (Fig. 3). We observed a significant decrease of the MAP in PC1/3 KO mice compared with WT mice after 60 min of LPS stimulation. Under identical conditions, no such blood pressure drop was observed in PC2 or PC7 KO mice. These results provide further evidence of PC1/3 null mice susceptibility to LPS-induced septic shock.

The most likely explanation for the drop in blood pressure as well as the susceptibility of PC1/3 KO mice to LPS is increased levels of cytokines. We therefore conducted time course experiments to determine the cytokine secretion profiles in the plasma, focusing at first on proinflammatory cytokines IL-6, TNF-α, and IL-1β. As expected in WT mice, IL-6 secretion in the plasma reached its peak after 4 h of LPS stimulation (Fig. 4*A*) followed by a return toward base-line concentrations 8 and 24 h following LPS stimulation. Similar secretion profiles were observed in the case of TNF-α and IL-1β in WT mouse plasma (Fig. 4, *B* and *C*).

However, the time course experiments from PC1/3 KO mice revealed a different profile of cytokine secretion. Four hours following LPS administration, we observed that in the PC1/3 KO mice the IL-6 plasma concentrations were 30 times greater than those measured in WT mice (Fig. 4*A*). Concentrations still increased about 2-fold at 8 h post-LPS stimulation in PC1/3 KO plasma instead of decreasing as seen in WT mice. In the case of TNF-α, recorded concentrations were 8 times higher in PC1/3 KO plasma compared with WT mice following 4 h of stimulation and continued to rise at 8 h, similar to IL-6 (Fig. 4*B*). IL-1β secretion in PC1/3 KO mice was also measured to be 5-fold higher than the concentration observed in WT mice 4 h post-LPS (Fig. 4*C*). Although concentrations decreased at 8 h of LPS stimulation in WT plasma, IL-1β secretion was 2 times greater in PC1/3 KO mice. No data could be obtained at the 24-h time point following LPS treatment as PC1/3 null mice did not survive.

As a comparative measure, we tested available PC2 and PC7 KO mice to determine whether those observed effects were PC1/3-specific. No significant differences were observed in the plasma cytokine profiles between KO and WT murine models for both PC2 and PC7 (Table 1). The time course analysis indicated an exaggerated proinflammatory cytokine response only in PC1/3 KO mice treated with LPS. This would suggest a role for PC1/3 in the regulation of proinflammatory cytokine secretion *in vivo*.

Expression of PC1/3 Gene in Peritoneal Macrophages—Macrophages are essential APCs in innate immunity because they are part of the first line of defense during an infection, and they are a major source of cytokine production. Although we have shown that the expression of PC1/3 co-localizes with the spleen macrophage marker CD14 (16), we wanted to establish clear evidence of PC1/3 expression in peritoneal macrophages. An RT-PCR was performed on peritoneal macrophage RNA,

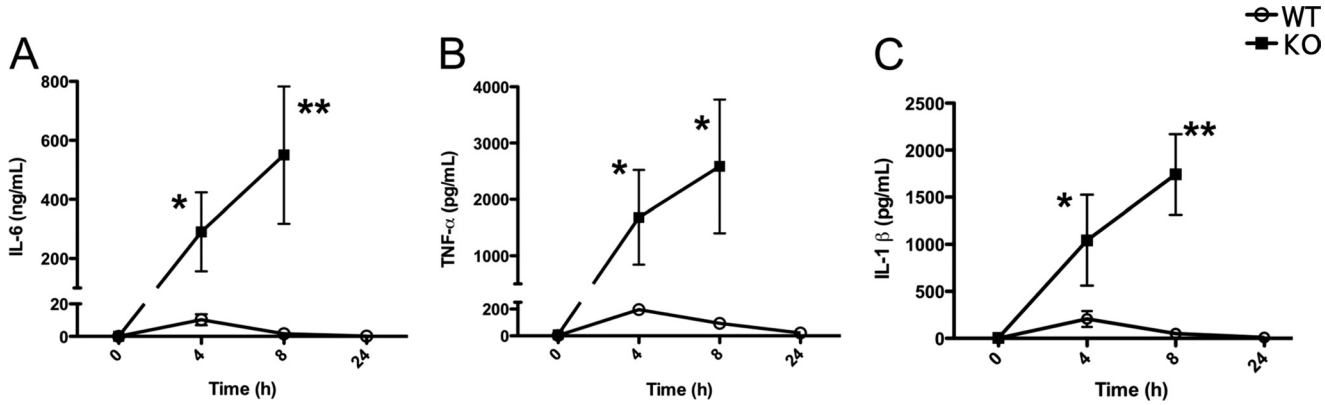

FIGURE 4. **Time course experiment of proinflammatory cytokines *in vivo*.** Concentrations of IL-6 (*A*), TNF-α (*B*), and IL-1β (*C*) were measured in the plasma collected from PC1/3 KO and WT mice injected intraperitoneally with 100 μg of LPS. PC1/3 KO mice were deceased following 24 h of LPS stimulation. Cytokine concentrations were measured using an ELISA kit. Data represent mean $\pm$ S.E. ($n = 4–7$; *, $p < 0.05$; **, $p < 0.01$).

TABLE 1

Effect of LPS administration on plasma cytokine concentrations in WT, PC2 KO, and PC7 KO mice

A comparison of proinflammatory cytokine concentrations secreted in PC2 KO and PC7 KO mice is shown. IL-6, IL-1β, and TNF-α were measured in the plasma of mice following intraperitoneal injection of 100 μg of LPS. Cytokines were measured in a time course experiment using an ELISA kit. Data represent mean $\pm$ S.E. ($n = 3–4$). ND, non-detected.

	PC2		PC7	
Cytokine	WT	KO	WT	KO
IL-6 (ng/ml)				
0 h	ND	ND	ND	ND
4 h	40 $\pm$ 20	20 $\pm$ 4	20 $\pm$ 10	30 $\pm$ 10
8 h	7 $\pm$ 4	5 $\pm$ 1	3 $\pm$ 2	5 $\pm$ 1
24 h	ND	ND	ND	ND
TNF-α (pg/ml)				
0 h	ND	ND	ND	ND
4 h	430 $\pm$ 110	290 $\pm$ 40	260 $\pm$ 50	780 $\pm$ 300
8 h	160 $\pm$ 60	90 $\pm$ 50	80 $\pm$ 30	110 $\pm$ 30
24 h	ND	ND	ND	ND
IL-1β (pg/ml)				
0 h	ND	ND	ND	ND
4 h	390 $\pm$ 180	150 $\pm$ 50	140 $\pm$ 40	150 $\pm$ 40
8 h	170 $\pm$ 160	50 $\pm$ 30	70 $\pm$ 20	100 $\pm$ 20
24 h	50 $\pm$ 40	ND	ND	9 $\pm$ 9

and the product was analyzed by gel electrophoresis. The observed band yielded the expected 252-bp cDNA fragment (Fig. 5*A*). Sequencing of the isolated cDNA confirmed its sequence, corresponding to nucleotides 80–331 of the PC1/3 mRNA (GenBank^{TM} accession number NM_013628.2). We next conducted a Western blot of proteins extracted from the pituitary gland from WT and KO mice to demonstrate the antibody specificity for PC1/3 (Fig. 5*B*, *panel a*). As expected, the specific PC1/3 band at ~84 kDa was observed in the WT but not in the KO mouse pituitary. A strong nonspecific band was always observed at ~90 kDa. We then analyzed (Fig. 5*B*, *panel b*) peritoneal macrophages in comparison with AtT-20 cells, which are known for their very high expression of PC1/3. The strong nonspecific band (~90 kDa) was again present (labeled with an *asterisk*), whereas the specific 84-kDa PC1/3 band was also observed with an identical migration pattern as that found in AtT-20 and WT pituitary positive controls. We conducted a mass spectrometry experiment to confirm the detection of PC1/3 in peritoneal macrophages. We used a gel LC-MS/MS approach. Membrane proteins extracted from LPS-stimulated or unstimulated WT and KO macrophages were resolved by SDS-PAGE, and bands corresponding to the approximate migration of PC1/3 were cut, trypsin-digested, and analyzed by LC-MS/MS on an LTQ-Orbitrap. We detected PC1/3 only in the WT LPS-stimulated sample. This may indicate that in the unstimulated sample the level of PC1/3 was below the detection limit of the technique. Fig. 5*C* shows the sequence of PC1/3 with *yellow* highlighted section representing the peptides detected by LC-MS/MS. Three unique peptides (Fig. 5*C*) of 95% PeptideProphet (49) probability were sequenced from three unique spectra (supplemental Fig. 1). A total of 10 spectra were assigned to PC1/3; all were from the same gel band. The ProteinProphet algorithm (50) assigned a probability for PC1/3 detection higher than 99.9% with a protein false discover rate lower than 0.01% and a peptide false discover rate of 1.1%. Those results validate the expression of PC1/3 at the protein level in peritoneal macrophages.

Effect of LPS Stimulation on Cytokine Production and Secretion in Primary PC1/3 KO Peritoneal Macrophages—WT macrophages secreted negligible basal amounts of proinflammatory cytokines, whereas LPS stimulation caused a significant increase in cytokine secretion (Fig. 6, *A–C*). PC1/3 KO macrophages also secreted low levels of cytokines when incubated with PBS; the exception was IL-1β, which was more significantly secreted by PC1/3 KO macrophages by about 2.5-fold compared with WT macrophages. LPS stimulation resulted in significantly amplified IL-6 and TNF-α secretion from primary PC1/3 KO macrophages compared with the WT cells. However, no significant difference was observed in IL-1β secretion after 4 h of LPS stimulation between PC1/3 KO and WT macrophages (Fig. 6*C*).

Intracellular proinflammatory cytokines were also analyzed in primary peritoneal macrophages following a 4-h LPS treatment (Fig. 6, *D–F*). In the presence of LPS, intracellular cytokine concentrations significantly increased compared with that of basal amounts both in WT and PC1/3 KO macrophages. No significant difference in cytokine concentrations was observed between WT and PC1/3 KO primary macrophages after LPS stimulation. Secretion and intracellular cytokine concentrations were also analyzed in PC2 KO and PC7 KO primary macrophages. No difference was observed in these models in comparison with WT macrophages stimulated with LPS.

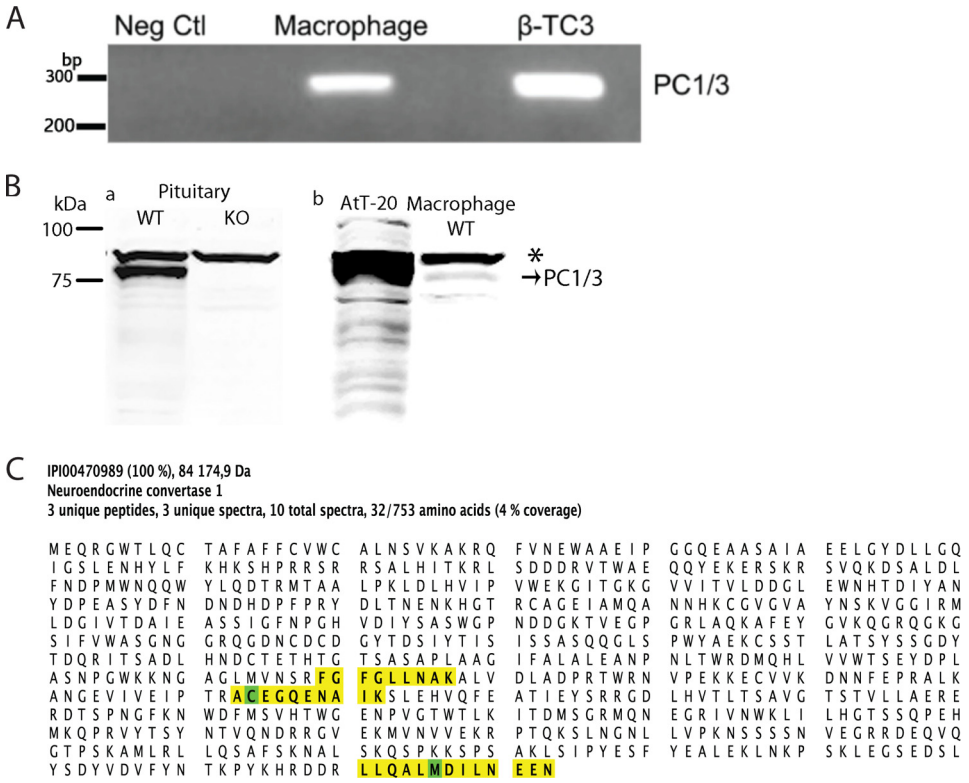

FIGURE 5. **Expression of PC1/3 gene in isolated peritoneal macrophages.** *A*, RT-PCR product was obtained using RNA extract from peritoneal macrophages and β-TC3 (positive control) that was then electrophoresed on a 1.5% agarose gel stained with ethidium bromide. A 252-bp fragment was observed in the macrophage sample, correlating with the expected length for PC1/3 gene. *B*, *panel a*, Western blot of 15 μg of protein extract from WT and PC1/3 KO mouse pituitary glands showing the specificity of the antibody. *Panel b*, Western blot of PC1/3 from 15 μg of isolated WT peritoneal macrophages. 15 μg of protein from mouse pituitary cells (AtT-20) was used as a positive control. The *asterisk* indicates a nonspecific band. *Neg Ctl*, negative control. *C*, evidence of expression of PC1/3 protein in peritoneal macrophages by mass spectrometry. Peritoneal macrophages were isolated from mice following 8-h treatment with intraperitoneal injection of 100 μg of LPS or saline. The membrane fraction was subjected to gel LC-MS/MS. PC1/3 was detected only in stimulated macrophage (99.9% probability) with three unique peptides (95% probability) from three unique spectra. A total of 10 spectra were assigned to PC1/3 with 4% protein coverage. *Yellow* highlighting represents assigned spectra, whereas *green* highlighting represents modified amino acids (oxidized methionine and alkylated cysteine).

Based on the sum of these data, we conclude that the lack of PC1/3 results in a deregulated cytokine secretion process with no observable effect on intracellular cytokines upon short term LPS stimulation. These *ex vivo* studies allowed us to identify an important role of PC1/3 in the control of the secretion of some proinflammatory cytokines (*e.g.* IL-6 and TNF-α) from LPS-treated macrophages.

We also tested the effects of LPS treatment of WT and PC1/3 KO mice on the expression profiles of the proinflammatory cytokine (IL-6, TNF-α, and IL-1β) mRNAs by RT-quantitative PCR. The relative gene expression was calculated by the ratio between RNA expression of stimulated macrophages (LPS) and that of the control macrophages (PBS). Only IL-6 mRNA was expressed at a higher level in both WT and PC1/3 KO LPS-stimulated primary macrophages. Still, no significant changes in relative gene expression were observed in all three cytokines between WT and PC1/3 KO macrophages stimulated with LPS (Fig. 7). These results indicate that PC1/3 does not seem to influence macrophage mRNA levels of IL-6, TNF-α, and IL-1β after 4-h LPS treatment.

Effect of PC1/3 KO on Cellular Structure of Isolated Peritoneal Macrophages—Because PC1/3 seems to play a role in cytokine secretion, we conducted a transmission electron microscopy experiment to determine whether structures involved in cytokine secretion and immune response could be affected by the absence of PC1/3. Peritoneal macrophages were isolated from WT and PC1/3 null mice following 8 h of stimulation with LPS or PBS (control) and then observed by TEM.

At first glance, the general structural aspects appeared to be similar when comparing macrophages from WT mice with those of PC1/3 KO mice (supplemental Fig. 2A). The shape and area of the nucleus were also comparable, indicative of the similarity of the cell population observed between each experimental condition (supplemental Fig. 2B). It has been reported that phagolysosome formation and secretory lysosome trafficking are important features for antigen presentation and cytokine response from APCs (45–47). This led us to conduct a detailed structural analysis of the macrophages by counting electron-dense vesicles (EDVs) (*i.e.* lysosomes, heterolysosomes, and storage vesicles) (Fig. 8*A*), vacuoles (*i.e.* events of pinocytosis, phagosomes, and phagolysosomes) (Fig. 8, *B* and *C*), and membrane projections, also known as pseudopods (Fig. 8*D*).

An expected LPS response was observed in WT macrophages (51) that resulted in a 3-fold increase in the ratio of phagolysosomal structures compared with the total amount of vacuoles as well as an enlargement of these compartments (Fig. 8*B*). The peripheral vacuole relative ratio compared with total vacuoles decreased 2-fold in LPS-stimulated WT macrophages (Fig. 8*C*).

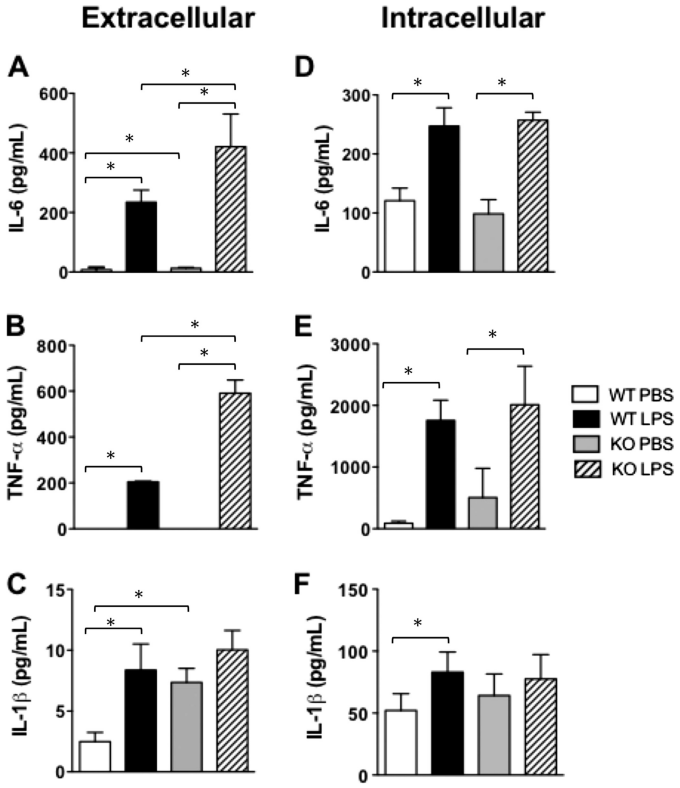

FIGURE 6. **Peritoneal macrophage content and secretion of proinflammatory cytokines.** Extracellular (*A–C*) and intracellular (*D–F*) proinflammatory cytokine concentrations were measured in isolated WT and PC1/3 KO peritoneal macrophages stimulated for 4 h with 100 ng/ml LPS or PBS. Cytokines were measured using an ELISA. Data represent mean ± S.E. ($n = 4$; *, $p < 0.05$).

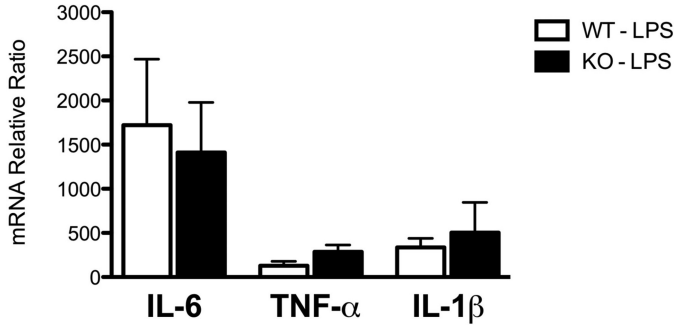

FIGURE 7. **Proinflammatory cytokine gene expression in peritoneal macrophages.** Proinflammatory cytokine mRNA expression in WT and PC1/3 KO macrophages stimulated for 4 h with 100 ng/ml LPS relative to the expression of these cytokines in control samples stimulated with saline is shown. mRNA was isolated from peritoneal macrophages and quantified by RT-quantitative PCR. All values were normalized to actin mRNA ($n = 3$). Data represent mean ± S.E.

At basal conditions, no change was observed in the total amount of vacuoles in all conditions observed (supplemental Fig. 1B). Also, no significant difference was observed in the ratio of peripheral (Fig. 8*C*), internal (data not shown), and phagolysosomal (Fig. 8*B*) vacuoles between WT and PC1/3 KO macrophages at basal conditions.

Stimulation with LPS caused an alternate structural organization in PC1/3 KO macrophages compared with the WT cells. As described previously, we observed a decrease in the number of peripheral vacuoles accompanied by an increase in the amount of phagolysosomes in WT macrophages following LPS stimulation. In fact, the ratio of peripheral vacuoles remained high in PC1/3 null macrophages (0.45 per cell), whereas the relative amounts of phagolysosomes were unaffected by the LPS stimulation.

We also examined the EDV characteristics following LPS stimulation. In WT macrophages, we observed a decrease in EDV optic densities after 8 h of LPS stimulation compared with control macrophages. Also, EDVs from LPS-stimulated WT macrophages were often located in or around vacuoles, which suggests that these vesicles released or were in the process of releasing their contents (Fig. 8*A*, *panel d*). An elevated amount of EDVs was observed in control PC1/3 KO macrophages compared with control WT cells (28 and 21 EDVs per cell, respectively) (Fig. 8*A*, *panel c*). Furthermore, the mean radius of EDVs measured at basal conditions in PC1/3 KO macrophages (0.24 nm) was larger than that observed in the WT macrophages (0.18 nm). Interestingly, LPS stimulation of macrophages caused a decrease in the amount of EDVs compared with the control cells, leveling the number of EDVs in LPS KO macrophages to the same level of LPS WT macrophages (14 EDVs per cell) (Fig. 8*A*, *panel e*). Also, differences in the morphology of EDVs were detected between PC1/3 KO and WT macrophages at basal conditions. In the former, EDVs appeared as round gray vesicles (Fig. 8*A*, *panel c*), whereas EDVs in WT macrophages had a heterogeneous content (Fig. 8*A*, *panels a* and *b*).

Further analysis was conducted to examine differences in membrane projections in macrophages because these structures are important indicators of cell activation and mediate vacuole formation via events of pinocytosis and phagocytosis. Under control and stimulated conditions, PC1/3 KO macrophages showed an increased number of membrane projections compared with WT macrophages with a respective increase of 1.3- and 1.7-fold per cell (Fig. 8*D*), suggesting an increased activation state in those cells. Taken together, these results demonstrate an abnormal structural phenotype of macrophages in the absence of PC1/3 that may affect cytokine secretion and trafficking as well as possible antigen presentation.

Implication of PC1/3 in T_h1/T_h2 Differentiation—An immune response *in vivo* involves the activity of both the innate and adaptive immune systems mediated by cells, such as macrophages. These cells can influence the differentiation of T_h cells to T_h1 or T_h2 cells to propagate a pro- or anti-inflammatory environment, respectively, which is determined mainly by the cytokine profile as well as antigen presentation. To study the effect of PC1/3 on T_h1/T_h2 differentiation, we used our murine model to perform an LPS stimulation time course and examined the plasma profile of IL-10, IL-12p70, and IFN-γ (Fig. 9). The IL-10 cytokine secretion profile shows a peak at 4 h post-LPS administration and levels returning to basal amounts at 24 h in WT mice. PC1/3 KO mice also show a peak of secretion at 4 h post-LPS that slightly decreased but failed to return to basal levels. At 8 h following LPS stimulation, the IL-10 plasma content in PC1/3 KO mice was significantly higher than in WT (Fig. 9*A*). These results suggest a failure in IL-10 feedback inhibition on PC1/3 KO innate immunity.

The IL-12p70 cytokine plasma content follows a profile similar to that of IL-10 in WT mice following LPS treatment over time. A peak at 4 h is also noted in PC1/3 KO mice with a significantly

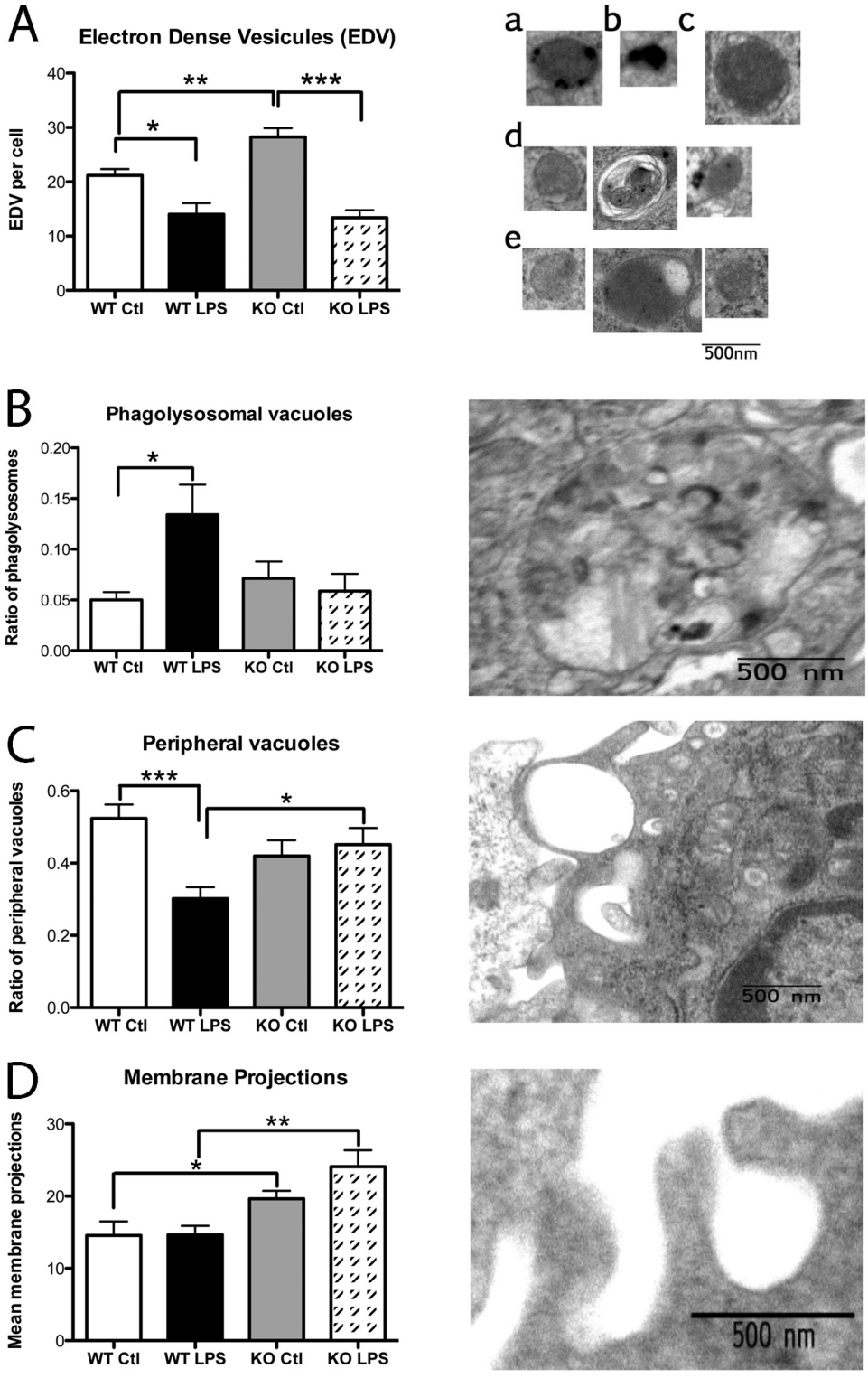

FIGURE 8. **Peritoneal macrophage structure observed by TEM.** Peritoneal macrophages isolated from WT and PC1/3 KO mice stimulated for 8 h with LPS or PBS (control (*Ctl*)) were analyzed by TEM. *A*, electron-dense vesicles were counted in control WT (*panels a* and *b*) and PC1/3 KO (*panel c*) as well as in LPS-stimulated WT (*panel d*) and PC1/3 KO (*panel e*) macrophages. The mean count per cell is reported on the graph. *B*, the ratio of phagolysosomal vacuoles was determined relative to the total amount of vacuoles. *C*, the ratio of peripheral vacuoles was calculated relative to the total vacuoles. *D*, the mean number of membrane projections per cell was calculated. Data represent mean ± S.E. ($n = 7–9$; *, $p < 0.05$; **, $p < 0.01$; ***, $p < 0.001$).

higher plasma concentration compared with WT mice. IL-12p70 levels decrease 8 h following LPS treatment in PC1/3 KO plasma but are still at a significantly higher level compared with WT mice (Fig. 9*B*). An increase in IL-12p70 secretion in PC1/3 KO mice favors proinflammatory T_h1 cell differentiation.

The IFN-γ profile concentration in the plasma following a time course of LPS treatment reveals a peak of secretion at 8 h in WT mice (Fig. 9*C*). PC1/3 KO and WT mice secrete similar levels of IFN-γ 4 h post-LPS stimulation. However, plasma contents soar at 8 h following LPS treatment to 30 times higher

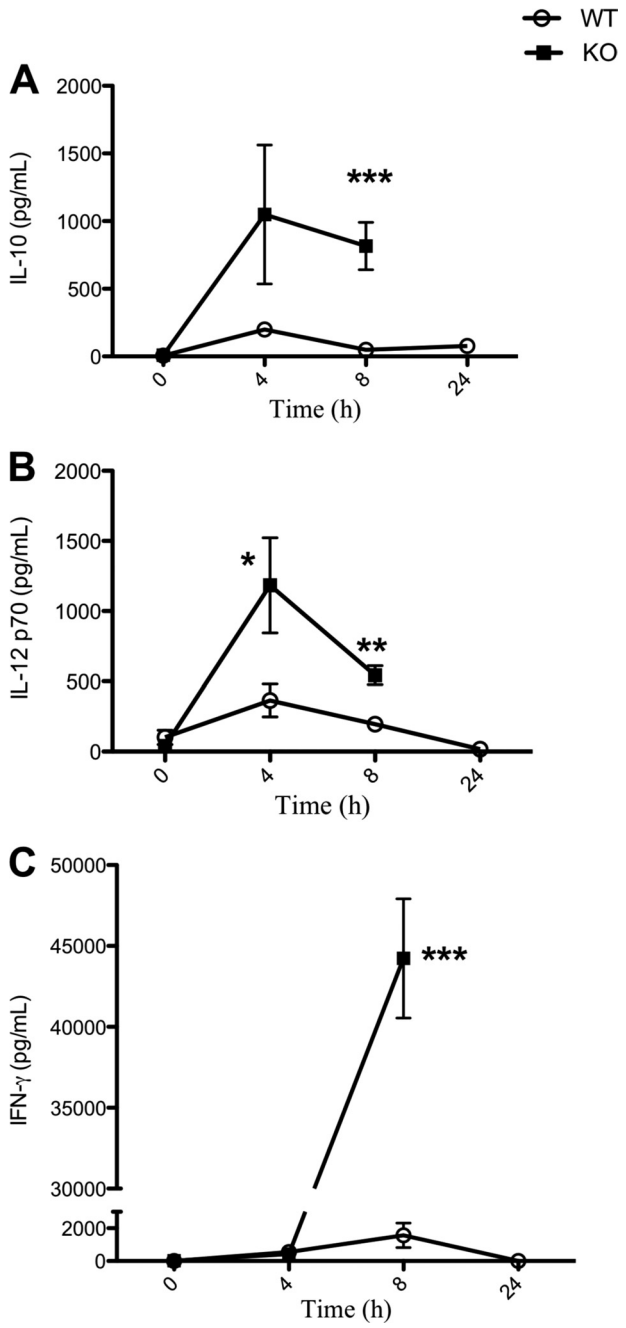

FIGURE 9. **Time course experiment of IL-10, IL-12, and IFN-γ cytokines *in vivo*.** The concentrations of IL-10 (*A*) and IL-12 (*B*), indicative of T_h2 and T_h1 differentiation, respectively, in WT and PC1/3 KO mice were measured in mouse plasma following 100-μg LPS stimulation administered intraperitoneally. *C*, IFN-γ, a proinflammatory cytokine secreted as a result of a T_h1 immune response, was also measured in a similar time course experiment. PC1/3 KO mice were deceased following 24 h of LPS stimulation. Cytokines were measured using ELISA kits specific for mouse IL-10, IL-12, and IFN-γ. Data represent mean ± S.E. ($n = 4–7$; *, $p < 0.05$; **, $p < 0.01$; ***, $p < 0.001$).

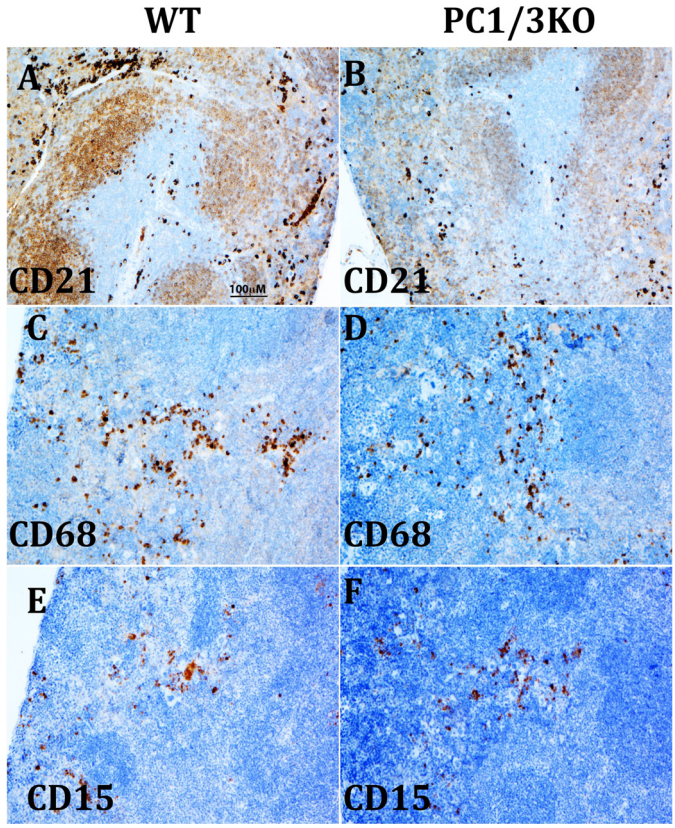

FIGURE 10. **Immunohistochemical staining of untreated WT and PC1/3 KO mouse spleens.** Labeling of dendritic cell CD21 (*A* and *B*), macrophage CD68 (*C* and *D*), and monocyte CD15 (*E* and *F*) is shown at a 10× magnification of the spleen.

than that observed in WT plasma contents (Fig. 9*C*). This 30-fold increase in IFN-γ secretion observed in PC1/3 KO mice provides further information of the proinflammatory cytokine profile secretion in these mice. This balance among IL-10, IL-12, and IFN-γ secretion profiles indicates that disruption of PC1/3 promotes T_h1 differentiation.

However, macrophages are not the only immune cells implicated in the induction of the T_h1 response. Dendritic cells also secrete IL-12 to favor T_h1 feedback during an immune reaction (52). Moreover, proper communication between APCs, T cells, and B cells is essential for the development of a T_h2 response and to provide negative feedback on the T_h1 response. We thus performed an immunohistochemical analysis with antibodies directed against immune "cluster differentiation" (CD) markers to determine the presence and distribution of these immune cells. As shown, PC1/3 KO has little or no effect on B, T, and natural killer cells (supplemental Figs. 3–5).

The marginal zone contains CD20, CD22, and IgM immunohistochemistry-positive B cell markers, whereas the nodes contain only CD22- and IgM-positive labeling (supplemental Fig. 2). This indicates that the absence of PC1/3 does not alter the trafficking of B cells in the spleen, which travel from the marginal zone to the white pulp node and then to the T cell zone (53). Both the T cells (CD3, CD4, and CD7) and natural killer T cells (CD56 and CD7) are present in the white pulp, specifically in the periarterial lymphatic sheath region, of PC1/3 null spleen but in a slightly lower amount compared with control spleens for some markers (WT) (supplemental Figs. 4 and 5). The highest impact observed is in regard to the localization of the follicular dendritic cells (CD21 and CD23 not shown), which have mostly disappeared from nodes and the marginal zone (Fig. 10, *A* and *B*), whereas macrophage (CD68) and monocyte (CD15) labeling remained unchanged (Fig. 10, *C–F*).

Therefore, a decrease of dendritic cells evokes the major contribution of macrophages in PC1/3 KO mice in swaying the T_h

immune reaction toward a proinflammatory response after LPS stimulation. The early and high secretion level of IL-12 further promotes INF-γ secretion by T cells and may outbalance the IL-10 negative feedback. These results contribute additional evidence that PC1/3 plays an essential role in the control of the proinflammatory immune response.

DISCUSSION

The use of KO mice has greatly contributed to elucidating the *in vivo* functions of a number of PCs (35, 36, 54–59). For PC1/3, the discovery of human deficiency cases (17, 60–63) has provided important data, which further instigated the development of KO animal models to study the physiological function of this enzyme (30). However, PC1/3 KO mouse studies have primarily focused on the study of the neuroendocrine functions of this convertase (17, 33, 34, 64). Because PC1/3 and PC2 are functionally closely related, studies on PC2 KO mice have also focused on its role in the neuroendocrine system (65, 66). However, few studies have provided evidence for PC1/3 expression in non-neuroendocrine cells, including macrophages (14, 15). Previous work from our laboratory has demonstrated that PC1/3 expression is regulated by pathogen-associated molecular patterns, specifically LPS, which activates the TLR4 pathway (16). The regulation of the observed expression pattern has encouraged us to explore the PC1/3 KO mouse model from a perspective relating to innate immune mechanisms.

In the present study, we report additional phenotypes in PC1/3 KO mice, such as an increase in the spleen size in these animals. We confirmed the expression of PC1/3 and for the first time observed the expression of proSAAS in the spleen. We also observed a spleen disorganization in PC1/3 null mice that was evident by the overlapping of specific compartments, such as the red pulp and the marginal zone. This chaotic phenotype may indicate a lack of proper communication between specific cell types, such as macrophages, B cells, and T cells, that may lead to an improper immune response (67, 68). Moreover, mice challenged with LPS showed an increase in proinflammatory cytokine secretion in the plasma and were much more susceptible to LPS-induced septic shock compared with WT mice. A decrease in MAP and a cytokine stormlike phenotype were detected in the plasma of these mice; both are clear evidence of septic shock (69). These observations suggest that in the spleen PC1/3 plays a role in innate immunity through, for example, the protection against an induced septic shock. We thus attempted to obtain further information about the function of PC1/3 at a cellular level within the PC1/3 KO mouse model.

APCs play an important role in initiating an immune response because they are responsible for the detection of pathogens, such as the recognition of LPS by TLR4, as well as communicating with the adaptive immune system by antigen presentation and cytokine secretion. Dendritic cells and macrophages are known to collaborate in this task by different cytokine profiles and modulation of adaptive and innate immunity (70). In the present study, spleen immunohistology showed a decrease in dendritic cell markers in PC1/3 KO mice compared with the WT, whereas the macrophage and monocyte markers were unchanged. Two different DC markers showed this reduction (*i.e.* CD21 and CD23), suggesting that the most likely explanation is a reduced DC population in the PC1/3 KO spleen. Because three types of DCs are present in the mouse spleen (71), it is difficult to ascertain whether this change is due to hematopoietic differentiation or a relocation of DCs to another lymphoid organ. Based on these and other findings, we hypothesize that the increased LPS sensitivity observed in the PC1/3 KO mice is ostensibly linked to macrophages. Indeed, in previous work, we demonstrated PC1/3 expression in splenic macrophages co-localized with CD14, a macrophage marker (16).

Because peritoneal macrophages are easily obtained, we used these as a cellular model to examine the role of PC1/3 in the macrophage. We established strong evidence that mouse peritoneal macrophages express PC1/3 by using RT-PCR, Western blotting, and mass spectrometry. This validated our cellular model to study the function of this enzyme in the macrophage.

Furthermore, we examined peritoneal macrophage morphological features. TEM experiments revealed that PC1/3 null macrophages showed a greater number of pseudopods under basal and 8-h LPS-stimulated conditions compared with the macrophages obtained from WT mice. Pseudopods are membrane extensions essential for sensing the environment, initiating phagocytosis, and mediating motility, hallmarks of macrophage activation (72, 73). Therefore, PC1/3 KO macrophages are primed in the absence of stimulation and remain active longer than the WT cells. We also demonstrated that PC1/3 KO macrophages secreted higher concentrations of proinflammatory cytokines; this correlates with the high levels observed in the plasma of these mice.

Because RNA expression levels were unchanged in the null macrophages following LPS treatment, we suggest that PC1/3 may be implicated in a downstream control of cytokine secretion. We also report that PC1/3 KO macrophages show a clear difference in EDV morphology and number as demonstrated in the TEM experiments, supporting our hypothesis. Indeed, heterogeneous contents were observed in WT cells, whereas homogenous EDVs were predominant in KO macrophages, implying that the contents of these vesicles differ. These EDVs are most likely secretory lysosomes or late endosomes known to be involved in the canonical (*e.g.* IL-6 and TNF-α) and non-canonical (*e.g.* IL-1β) secretion pathways of cytokines (74–76). In addition, our data show that IL-1β secretion is increased in non-stimulated PC1/3 KO macrophages as compared with WT; this fits with the well established data that IL-1β secretion bypasses the trans-Golgi network (76). In contrast, PC1/3 does not appear to affect the trans-Golgi network retention of cytokines like TNF-α but rather changes the cytokine turnover in post-Golgi transport vesicles upon stimulation. The sum of these data supports a role for PC1/3 in the regulation of vesicle trafficking in macrophages, which contributes to the observed phenotype when PC1/3 is disrupted in the KO mouse model.

The question that remains to be answered is the mechanism by which PC1/3 regulates cytokine secretion. It is known that PC1/3 sorting to the regulated secretory pathway depends on its C terminus, which contains an amphipathic and hydrophobic α-helix that anchors the enzyme at the site of formation of dense core secretory granules in the trans-Golgi network (77). Some studies have implicated PC1/3 as a possible chaperone for

proteins to the dense core secretory granules by binding the recognition cleavage site composed of paired basic amino acids (78). Adaptor molecules, such as EpsinR, are crucial for the sorting of proteins in the recycling endosomes (79) and contain the recognition sequence required to bind PC1/3. Therefore, we speculate that PC1/3 could regulate cytokine secretion by directing trafficking chaperones while affecting the cytokine secretion and turnover.

An alternative hypothesis would be that PC1/3 affects secretion through cleavage of one or more substrates. Because we only showed the full-length form of PC1/3, and the activity of this full-length form has been demonstrated previously, it remains likely that processing activity could impact secretion. It is noted that full-length PC1/3 does not require an acidic environment to be active (80). We cannot exclude that the shorter forms of PC1/3 are also present in peritoneal macrophages; however, others have shown a shorter form (*i.e.* 66 kDa) in alveolar macrophages and spleen monocytes (15). It is well established that the immune and neuroendocrine systems communicate with each other in a paracrine way (17, 81, 82). The role of neuropeptides as secretion modulators is well known. For example, neuropeptide Y was shown to modulate IL-6 secretion from macrophages (83), and opioids are known to induce signaling in immune cells We have demonstrated previously that neuropeptides, such as enkephalin, are co-expressed with PC1/3 in the spleen (16). Others have also observed enkephalin peptides in immune cells and showed that PC1/3 expression leads to the formation of longer peptides (15). Neuropeptides expressed in immune cells could have autocrine activity that regulates secretion. The identification of cognate PC1/3 substrates in macrophages remains an important challenge to better define the mechanisms involved.

Another interesting phenotype observed in the PC1/3 null mice is the global $CD4^+$ T_h1-like response to LPS as evident by the massive secretion of IFN-γ, which is indicative of a proinflammatory pathway (84). M1 and M2 macrophages are known for their capacity to activate T_h1 and T_h2 cells, respectively (70). The M1 macrophages secrete IL-12 to activate the T_h1 cell to promote a proinflammatory response (85). However, LPS alone generally stimulates a T_h2 response, leading to protection against LPS toxicity with an inflammatory cytokine profile (*e.g.* IL-1β, IL-6, and TNF-α) controlled by IL-10 (86). The secretion of IL-10 inhibits both the macrophage proinflammatory activities and T_h1 differentiation (27, 84). However, co-stimulation of macrophages with LPS and IFN-γ gives rise to an M1 response (87, 88). We show that IL-10 is highly secreted in the PC1/3 KO mouse plasma following LPS stimulation; however, INF-γ and IL-12 still surge in PC1/3 null mice, indicating a failure of IL-10 to properly inhibit macrophage proinflammatory activities. The high INF-γ and rapid IL-12 oversecretion observed in PC1/3 null mice may initiate a positive feedback to further activate the M1 macrophage proinflammatory activities and inhibit T_h2 differentiation (89). This would correlate with the observed time course of IL-10 where at 8 h post-LPS the IL-10 concentration decreases slightly as the amount of IFN-γ increases dramatically. Interestingly, INF-γ is produced by T_h1 (90) cells, and it is known that IL-10 regulation of macrophages involves regulatory T cells (84, 91). We can thus speculate that PC1/3 would directly or indirectly regulate cytokine secretion in other immune cells, which would contribute to the observed KO mice phenotype.

Apart from the cytokine profile, antigen presentation is also imperative in regulating the T_h1 and T_h2 pathways. By examining once more the macrophages by TEM, PC1/3 KO macrophages were shown to have a reduced capacity to form phagolysosomes following 8-h LPS stimulation. Although phagocytosis appears to be performed efficiently in WT macrophages because we observed an increase in phagolysosomal vacuoles accompanied by a decrease in peripheral vacuoles, this pattern of vacuoles is present to a lesser degree in the PC1/3 KO macrophages. This suggests a change in phagocytosis processing in these cells that may affect many features of the LPS immune response, such as antigen presentation (92). This change in the phagocytosis pathway may indicate an increase TLR4 signaling because it was shown that TLR4 slows the rate of phagolysosome fusion (93). Also, this simple default in lysosome trafficking can contribute to a "cytokine stormlike" phenotype as reported in the RAB7 KO mouse model (94).

In conclusion, our study has provided evidence for a novel role of PC1/3 in macrophages by regulating proinflammatory immune responses. Because many diseases are related to the APC response and their related T cell balance in cancer (95, 96), autoimmune diseases (97), and chronic allergy (98), exploring the role of PC1/3 in immunity may lead to novel insights in these diseases. The development of better tools to study the role of PC1/3 in immune cells and tissues is now justified. The use of conditional KO would be necessary to rule out any paracrine effects from other PC1/3-expressing cells and tissues on immune cells. Also the use of human macrophage-derived cell lines, such as THP-1, which expresses PC1/3 (14), would be an interesting model to establish the link between the function of PC1/3 in human and mouse immune cells. These would greatly contribute to the advancement in the identification of molecular mechanisms and pathways by which PC1/3 regulates cytokine secretion.

Acknowledgments—We thank Dany Gauthier for technical expertise and Denis Faubert for LC-MS/MS analyses.

REFERENCES

1. Rholam, M., and Fahy, C. (2009) Processing of peptide and hormone precursors at the dibasic cleavage sites. *Cell. Mol. Life Sci.* **66,** 2075–2091
2. Seidah, N. G., and Chrétien, M. (1999) Proprotein and prohormone convertases: a family of subtilases generating diverse bioactive polypeptides. *Brain Res.* **848,** 45–62
3. Hosaka, M., Nagahama, M., Kim, W. S., Watanabe, T., Hatsuzawa, K., Ikemizu, J., Murakami, K., and Nakayama, K. (1991) Arg-*X*-Lys/Arg-Arg motif as a signal for precursor cleavage catalyzed by furin within the constitutive secretory pathway. *J. Biol. Chem.* **266,** 12127–12130
4. Seidah, N. G., Khatib, A. M., and Prat, A. (2006) The proprotein convertases and their implication in sterol and/or lipid metabolism. *Biol. Chem.* **387,** 871–877
5. Siezen, R. J., and Leunissen, J. A. (1997) Subtilases: the superfamily of subtilisin-like serine proteases. *Protein Sci.* **6,** 501–523
6. Creemers, J. W., Siezen, R. J., Roebroek, A. J., Ayoubi, T. A., Huylebroeck, D., and Van de Ven, W. J. (1993) Modulation of furin-mediated proprotein processing activity by site-directed mutagenesis. *J. Biol. Chem.* **268,** 21826–21834

7. Creemers, J. W., Vey, M., Schäfer, W., Ayoubi, T. A., Roebroek, A. J., Klenk, H. D., Garten, W., and Van de Ven, W. J. (1995) Endoproteolytic cleavage of its propeptide is a prerequisite for efficient transport of furin out of the endoplasmic reticulum. *J. Biol. Chem.* **270,** 2695–2702
8. Essalmani, R., Zaid, A., Marcinkiewicz, J., Chamberland, A., Pasquato, A., Seidah, N. G., and Prat, A. (2008) *In vivo* functions of the proprotein convertase PC5/6 during mouse development: Gdf11 is a likely substrate. *Proc. Natl. Acad. Sci. U.S.A.* **105,** 5750–5755
9. Nakayama, K. (1997) Furin: a mammalian subtilisin/Kex2p-like endoprotease involved in processing of a wide variety of precursor proteins. *Biochem. J.* **327,** 625–635
10. Seidah, N. G., Day, R., Marcinkiewicz, M., and Chrétien, M. (1998) Precursor convertases: an evolutionary ancient, cell-specific, combinatorial mechanism yielding diverse bioactive peptides and proteins. *Ann. N.Y. Acad. Sci.* **839,** 9–24
11. Portela-Gomes, G. M., Grimelius, L., and Stridsberg, M. (2008) Prohormone convertases 1/3, 2, furin and protein 7B2 (Secretogranin V) in endocrine cells of the human pancreas. *Regul. Pept.* **146,** 117–124
12. Schäfer, M. K., Day, R., Cullinan, W. E., Chrétien, M., Seidah, N. G., and Watson, S. J. (1993) Gene expression of prohormone and proprotein convertases in the rat CNS: a comparative *in situ* hybridization analysis. *J. Neurosci.* **13,** 1258–1279
13. Day, R., Schafer, M. K., Watson, S. J., Chrétien, M., and Seidah, N. G. (1992) Distribution and regulation of the prohormone convertases PC1 and PC2 in the rat pituitary. *Mol. Endocrinol.* **6,** 485–497
14. LaMendola, J., Martin, S. K., and Steiner, D. F. (1997) Expression of PC3, carboxypeptidase E and enkephalin in human monocyte-derived macrophages as a tool for genetic studies. *FEBS Lett.* **404,** 19–22
15. Vindrola, O., Mayer, A. M., Citera, G., Spitzer, J. A., and Espinoza, L. R. (1994) Prohormone convertases PC2 and PC3 in rat neutrophils and macrophages. Parallel changes with proenkephalin-derived peptides induced by LPS *in vivo*. *Neuropeptides* **27,** 235–244
16. Lansac, G., Dong, W., Dubois, C. M., Benlarbi, N., Afonso, C., Fournier, I., Salzet, M., and Day, R. (2006) Lipopolysaccharide mediated regulation of neuroendocrine associated proprotein convertases and neuropeptide precursor processing in the rat spleen. *J. Neuroimmunol.* **171,** 57–71
17. Salzet, M., Vieau, D., and Day, R. (2000) Crosstalk between nervous and immune systems through the animal kingdom: focus on opioids. *Trends Neurosci.* **23,** 550–555
18. Salzet, M. (2001) Neuroimmunology of opioids from invertebrates to human. *Neuro Endocrinol. Lett.* **22,** 467–474
19. Day, R., and Salzet, M. (2002) The neuroendocrine phenotype, cellular plasticity, and the search for genetic switches: redefining the diffuse neuroendocrine system. *Neuro Endocrinol. Lett.* **23,** 447–451
20. Akira, S., Takeda, K., and Kaisho, T. (2001) Toll-like receptors: critical proteins linking innate and acquired immunity. *Nat. Immunol.* **2,** 675–680
21. Lu, Y. C., Yeh, W. C., and Ohashi, P. S. (2008) LPS/TLR4 signal transduction pathway. *Cytokine* **42,** 145–151
22. Chow, J. C., Young, D. W., Golenbock, D. T., Christ, W. J., and Gusovsky, F. (1999) Toll-like receptor-4 mediates lipopolysaccharide-induced signal transduction. *J. Biol. Chem.* **274,** 10689–10692
23. Rautajoki, K. J., Kylaniemi, M. K., Raghav, S. K., Rao, K., and Lahesmaa, R. (2008) An insight into molecular mechanisms of human T helper cell differentiation. *Ann. Med.* **40,** 322–335
24. Cottrez, F., Hurst, S. D., Coffman, R. L., and Groux, H. (2000) T regulatory cells 1 inhibit a Th2-specific response in vivo. *J. Immunol.* **165,** 4848–4853
25. Schroder, K., Sweet, M. J., and Hume, D. A. (2006) Signal integration between IFNγ and TLR signalling pathways in macrophages. *Immunobiology* **211,** 511–524
26. Puddu, P., Fantuzzi, L., Borghi, P., Varano, B., Rainaldi, G., Guillemard, E., Malorni, W., Nicaise, P., Wolf, S. F., Belardelli, F., and Gessani, S. (1997) IL-12 induces IFN-γ expression and secretion in mouse peritoneal macrophages. *J. Immunol.* **159,** 3490–3497
27. Fiorentino, D. F., Zlotnik, A., Mosmann, T. R., Howard, M., and O'Garra, A. (1991) IL-10 inhibits cytokine production by activated macrophages. *J. Immunol.* **147,** 3815–3822
28. Kohyama, M., Ise, W., Edelson, B. T., Wilker, P. R., Hildner, K., Mejia, C., Frazier, W. A., Murphy, T. L., and Murphy, K. M. (2009) Role for Spi-C in the development of red pulp macrophages and splenic iron homeostasis. *Nature* **457,** 318–321
29. Miyake, K. (2003) Innate recognition of lipopolysaccharide by CD14 and toll-like receptor 4-MD-2: unique roles for MD-2. *Int. Immunopharmacol.* **3,** 119–128
30. Zhu, X., Zhou, A., Dey, A., Norrbom, C., Carroll, R., Zhang, C., Laurent, V., Lindberg, I., Ugleholdt, R., Holst, J. J., and Steiner, D. F. (2002) Disruption of PC1/3 expression in mice causes dwarfism and multiple neuroendocrine peptide processing defects. *Proc. Natl. Acad. Sci. U.S.A.* **99,** 10293–10298
31. Dey, A., Xhu, X., Carroll, R., Turck, C. W., Stein, J., and Steiner, D. F. (2003) Biological processing of the cocaine and amphetamine-regulated transcript precursors by prohormone convertases, PC2 and PC1/3. *J. Biol. Chem.* **278,** 15007–15014
32. Marzban, L., Trigo-Gonzalez, G., Zhu, X., Rhodes, C. J., Halban, P. A., Steiner, D. F., and Verchere, C. B. (2004) Role of β-cell prohormone convertase (PC)1/3 in processing of pro-islet amyloid polypeptide. *Diabetes* **53,** 141–148
33. Ugleholdt, R., Poulsen, M. L., Holst, P. J., Irminger, J. C., Orskov, C., Pedersen, J., Rosenkilde, M. M., Zhu, X., Steiner, D. F., and Holst, J. J. (2006) Prohormone convertase 1/3 is essential for processing of the glucose-dependent insulinotropic polypeptide precursor. *J. Biol. Chem.* **281,** 11050–11057
34. Wardman, J. H., Zhang, X., Gagnon, S., Castro, L. M., Zhu, X., Steiner, D. F., Day, R., and Fricker, L. D. (2010) Analysis of peptides in prohormone convertase 1/3 null mouse brain using quantitative peptidomics. *J. Neurochem.* **114,** 215–225
35. Furuta, M., Yano, H., Zhou, A., Rouillé, Y., Holst, J. J., Carroll, R., Ravazzola, M., Orci, L., Furuta, H., and Steiner, D. F. (1997) Defective prohormone processing and altered pancreatic islet morphology in mice lacking active SPC2. *Proc. Natl. Acad. Sci. U.S.A.* **94,** 6646–6651
36. Villeneuve, P., Feliciangeli, S., Croissandeau, G., Seidah, N. G., Mbikay, M., Kitabgi, P., and Beaudet, A. (2002) Altered processing of the neurotensin/neuromedin N precursor in PC2 knock down mice: a biochemical and immunohistochemical study. *J. Neurochem.* **82,** 783–793
37. D'Anjou, F., Routhier, S., Perreault, J. P., Latil, A., Bonnel, D., Fournier, I., Salzet, M., and Day, R. (2011) Molecular validation of PACE4 as a target in prostate cancer. *Transl. Oncol.* **4,** 157–172
38. Wardman, J. H., Berezniuk, I., Di, S., Tasker, J. G., and Fricker, L. D. (2011) ProSAAS-derived peptides are colocalized with neuropeptide Y and function as neuropeptides in the regulation of food intake. *PLoS One* **6,** e28152
39. Grenier, C., Bissonnette, C., Volkov, L., and Roucou, X. (2006) Molecular morphology and toxicity of cytoplasmic prion protein aggregates in neuronal and non-neuronal cells. *J. Neurochem.* **97,** 1456–1466
40. Benjannet, S., Rondeau, N., Paquet, L., Boudreault, A., Lazure, C., Chrétien, M., and Seidah, N. G. (1993) Comparative biosynthesis, covalent post-translational modifications and efficiency of prosegment cleavage of the prohormone convertases PC1 and PC2: glycosylation, sulphation and identification of the intracellular site of prosegment cleavage of PC1 and PC2. *Biochem. J.* **294,** 735–743
41. Polati, R., Castagna, A., Bossi, A., Campostrini, N., Zaninotto, F., Timperio, A. M., Zolla, L., Olivieri, O., Corrocher, R., and Girelli, D. (2009) High resolution preparation of monocyte-derived macrophages (MDM) protein fractions for clinical proteomics. *Proteome Sci.* **7,** 4
42. Havlis, J., Thomas, H., Sebela, M., and Shevchenko, A. (2003) Fast-response proteomics by accelerated in-gel digestion of proteins. *Anal. Chem.* **75,** 1300–1306
43. Cesta, M. F. (2006) Normal structure, function, and histology of the spleen. *Toxicol. Pathol.* **34,** 455–465
44. You, Y., Myers, R. C., Freeberg, L., Foote, J., Kearney, J. F., Justement, L. B., and Carter, R. H. (2011) Marginal zone B cells regulate antigen capture by marginal zone macrophages. *J. Immunol.* **186,** 2172–2181
45. Jia, T., and Pamer, E. G. (2009) Immunology. Dispensable but not irrelevant. *Science* **325,** 549–550
46. Takahashi, K., Shibata, T., Akashi-Takamura, S., Kiyokawa, T., Wakabayashi, Y., Tanimura, N., Kobayashi, T., Matsumoto, F., Fukui, R., Kouro,

T., Nagai, Y., Takatsu, K., Saitoh, S., and Miyake, K. (2007) A protein associated with Toll-like receptor (TLR) 4 (PRAT4A) is required for TLR-dependent immune responses. *J. Exp. Med.* **204,** 2963–2976
47. MacMicking, J. D., Nathan, C., Hom, G., Chartrain, N., Fletcher, D. S., Trumbauer, M., Stevens, K., Xie, Q. W., Sokol, K., Hutchinson, N., Chen, H., and Mudget, J. S. (1995) Altered responses to bacterial infection and endotoxic shock in mice lacking inducible nitric oxide synthase. *Cell* **81,** 641–650
48. Sriskandan, S., and Altmann, D. M. (2008) The immunology of sepsis. *J. Pathol.* **214,** 211–223
49. Keller, A., Nesvizhskii, A. I., Kolker, E., and Aebersold, R. (2002) Empirical statistical model to estimate the accuracy of peptide identifications made by MS/MS and database search. *Anal. Chem.* **74,** 5383–5392
50. Nesvizhskii, A. I., Keller, A., Kolker, E., and Aebersold, R. (2003) A statistical model for identifying proteins by tandem mass spectrometry. *Anal. Chem.* **75,** 4646–4658
51. Nacife, V. P., Soeiro Mde, N., Gomes, R. N., D'Avila, H., Castro-Faria Neto, H. C., and Meirelles Mde, N. (2004) Morphological and biochemical characterization of macrophages activated by carrageenan and lipopolysaccharide *in vivo*. *Cell Struct. Funct.* **29,** 27–34
52. Moser, M., and Murphy, K. M. (2000) Dendritic cell regulation of TH1-TH2 development. *Nat. Immunol.* **1,** 199–205
53. Mebius, R. E., and Kraal, G. (2005) Structure and function of the spleen. *Nat. Rev. Immunol.* **5,** 606–616
54. Roebroek, A. J., Umans, L., Pauli, I. G., Robertson, E. J., van Leuven, F., Van de Ven, W. J., and Constam, D. B. (1998) Failure of ventral closure and axial rotation in embryos lacking the proprotein convertase furin. *Development* **125,** 4863–4876
55. Mbikay, M., Tadros, H., Ishida, N., Lerner, C. P., De Lamirande, E., Chen, A., El-Alfy, M., Clermont, Y., Seidah, N. G., Chrétien, M., Gagnon, C., and Simpson, E. M. (1997) Impaired fertility in mice deficient for the testicular germ-cell protease PC4. *Proc. Natl. Acad. Sci. U.S.A.* **94,** 6842–6846
56. Constam, D. B., and Robertson, E. J. (2000) SPC4/PACE4 regulates a TGFβ signaling network during axis formation. *Genes Dev.* **14,** 1146–1155
57. Essalmani, R., Hamelin, J., Marcinkiewicz, J., Chamberland, A., Mbikay, M., Chrétien, M., Seidah, N. G., and Prat, A. (2006) Deletion of the gene encoding proprotein convertase 5/6 causes early embryonic lethality in the mouse. *Mol. Cell. Biol.* **26,** 354–361
58. Yang, J., Goldstein, J. L., Hammer, R. E., Moon, Y. A., Brown, M. S., and Horton, J. D. (2001) Decreased lipid synthesis in livers of mice with disrupted Site-1 protease gene. *Proc. Natl. Acad. Sci. U.S.A.* **98,** 13607–13612
59. Abifadel, M., Varret, M., Rabès, J. P., Allard, D., Ouguerram, K., Devillers, M., Cruaud, C., Benjannet, S., Wickham, L., Erlich, D., Derré, A., Villéger, L., Farnier, M., Beucler, I., Bruckert, E., Chambaz, J., Chanu, B., Lecerf, J. M., Luc, G., Moulin, P., Weissenbach, J., Prat, A., Krempf, M., Junien, C., Seidah, N. G., and Boileau, C. (2003) Mutations in PCSK9 cause autosomal dominant hypercholesterolemia. *Nat. Genet.* **34,** 154–156
60. O'Rahilly, S., Gray, H., Humphreys, P. J., Krook, A., Polonsky, K. S., White, A., Gibson, S., Taylor, K., and Carr, C. (1995) Brief report: impaired processing of prohormones associated with abnormalities of glucose homeostasis and adrenal function. *N. Engl. J. Med.* **333,** 1386–1390
61. Jackson, R. S., Creemers, J. W., Ohagi, S., Raffin-Sanson, M. L., Sanders, L., Montague, C. T., Hutton, J. C., and O'Rahilly, S. (1997) Obesity and impaired prohormone processing associated with mutations in the human prohormone convertase 1 gene. *Nat. Genet.* **16,** 303–306
62. Jackson, R. S., Creemers, J. W., Farooqi, I. S., Raffin-Sanson, M. L., Varro, A., Dockray, G. J., Holst, J. J., Brubaker, P. L., Corvol, P., Polonsky, K. S., Ostrega, D., Becker, K. L., Bertagna, X., Hutton, J. C., White, A., Dattani, M. T., Hussain, K., Middleton, S. J., Nicole, T. M., Milla, P. J., Lindley, K. J., and O'Rahilly, S. (2003) Small-intestinal dysfunction accompanies the complex endocrinopathy of human proprotein convertase 1 deficiency. *J. Clin. Investig.* **112,** 1550–1560
63. Farooqi, I. S., Volders, K., Stanhope, R., Heuschkel, R., White, A., Lank, E., Keogh, J., O'Rahilly, S., and Creemers, J. W. (2007) Hyperphagia and early-onset obesity due to a novel homozygous missense mutation in prohormone convertase 1/3. *J. Clin. Endocrinol. Metab.* **92,** 3369–3373
64. Ugleholdt, R., Zhu, X., Deacon, C. F., Ørskov, C., Steiner, D. F., and Holst, J. J. (2004) Impaired intestinal proglucagon processing in mice lacking prohormone convertase 1. *Endocrinology* **145,** 1349–1355
65. Furuta, M., Zhou, A., Webb, G., Carroll, R., Ravazzola, M., Orci, L., and Steiner, D. F. (2001) Severe defect in proglucagon processing in islet A-cells of prohormone convertase 2 null mice. *J. Biol. Chem.* **276,** 27197–27202
66. Pan, H., Che, F. Y., Peng, B., Steiner, D. F., Pintar, J. E., and Fricker, L. D. (2006) The role of prohormone convertase-2 in hypothalamic neuropeptide processing: a quantitative neuropeptidomic study. *J. Neurochem.* **98,** 1763–1777
67. Pasparakis, M., Alexopoulou, L., Episkopou, V., and Kollias, G. (1996) Immune and inflammatory responses in TNFα-deficient mice: a critical requirement for TNFα in the formation of primary B cell follicles, follicular dendritic cell networks and germinal centers, and in the maturation of the humoral immune response. *J. Exp. Med.* **184,** 1397–1411
68. Tumanov, A. V., Grivennikov, S. I., Shakhov, A. N., Rybtsov, S. A., Koroleva, E. P., Takeda, J., Nedospasov, S. A., and Kuprash, D. V. (2003) Dissecting the role of lymphotoxin in lymphoid organs by conditional targeting. *Immunol. Rev.* **195,** 106–116
69. Rittirsch, D., Flierl, M. A., and Ward, P. A. (2008) Harmful molecular mechanisms in sepsis. *Nat. Rev. Immunol.* **8,** 776–787
70. Zanoni, I., and Granucci, F. (2009) Dendritic cells and macrophages: same receptors but different functions. *Curr. Immunol. Rev.* **5,** 311–325
71. Kamath, A. T., Pooley, J., O'Keeffe, M. A., Vremec, D., Zhan, Y., Lew, A. M., D'Amico, A., Wu, L., Tough, D. F., and Shortman, K. (2000) The development, maturation, and turnover rate of mouse spleen dendritic cell populations. *J. Immunol.* **165,** 6762–6770
72. Rittig, M. G., Wilske, B., and Krause, A. (1999) Phagocytosis of microorganisms by means of overshooting pseudopods: where do we stand? *Microbes Infect.* **1,** 727–735
73. Isaac, B. M., Ishihara, D., Nusblat, L. M., Gevrey, J. C., Dovas, A., Condeelis, J., and Cox, D. (2010) N-WASP has the ability to compensate for the loss of WASP in macrophage podosome formation and chemotaxis. *Exp. Cell Res.* **316,** 3406–3416
74. Blott, E. J., and Griffiths, G. M. (2002) Secretory lysosomes. *Nat. Rev. Mol. Cell Biol.* **3,** 122–131
75. Duitman, E. H., Orinska, Z., and Bulfone-Paus, S. (2011) Mechanisms of cytokine secretion: a portfolio of distinct pathways allows flexibility in cytokine activity. *Eur. J. Cell Biol.* **90,** 476–483
76. Stow, J. L., Low, P. C., Offenhäuser, C., and Sangermani, D. (2009) Cytokine secretion in macrophages and other cells: pathways and mediators. *Immunobiology* **214,** 601–612
77. Dikeakos, J. D., Di Lello, P., Lacombe, M. J., Ghirlando, R., Legault, P., Reudelhuber, T. L., and Omichinski, J. G. (2009) Functional and structural characterization of a dense core secretory granule sorting domain from the PC1/3 protease. *Proc. Natl. Acad. Sci. U.S.A.* **106,** 7408–7413
78. Dikeakos, J. D., and Reudelhuber, T. L. (2007) Sending proteins to dense core secretory granules: still a lot to sort out. *J. Cell Biol.* **177,** 191–196
79. Saint-Pol, A., Yélamos, B., Amessou, M., Mills, I. G., Dugast, M., Tenza, D., Schu, P., Antony, C., McMahon, H. T., Lamaze, C., and Johannes, L. (2004) Clathrin adaptor epsinR is required for retrograde sorting on early endosomal membranes. *Dev. Cell* **6,** 525–538
80. Jean, F., Basak, A., Rondeau, N., Benjannet, S., Hendy, G. N., Seidah, N. G., Chrétien, M., and Lazure, C. (1993) Enzymic characterization of murine and human prohormone convertase-1 (mPC1 and hPC1) expressed in mammalian GH4C1 cells. *Biochem. J.* **292,** 891–900
81. Haddad, J. J., Saadé, N. E., and Safieh-Garabedian, B. (2002) Cytokines and neuro-immune-endocrine interactions: a role for the hypothalamic-pituitary-adrenal revolving axis. *J. Neuroimmunol.* **133,** 1–19
82. Sternberg, E. M. (2006) Neural regulation of innate immunity: a coordinated nonspecific host response to pathogens. *Nat. Rev. Immunol.* **6,** 318–328
83. Straub, R. H., Schaller, T., Miller, L. E., von Hörsten, S., Jessop, D. S., Falk, W., and Schölmerich, J. (2000) Neuropeptide Y cotransmission with norepinephrine in the sympathetic nerve-macrophage interplay. *J. Neurochem.* **75,** 2464–2471
84. Cope, A., Le Friec, G., Cardone, J., and Kemper, C. (2011) The Th1 life cycle: molecular control of IFN-γ to IL-10 switching. *Trends Immunol.* **32,**

278–286
85. Hsieh, C. S., Macatonia, S. E., Tripp, C. S., Wolf, S. F., O'Garra, A., and Murphy, K. M. (1993) Development of TH1 $CD4^+$ T cells through IL-12 produced by *Listeria*-induced macrophages. *Science* **260,** 547–549
86. Anderson, C. F., and Mosser, D. M. (2002) Cutting edge: biasing immune responses by directing antigen to macrophage Fcγ receptors. *J. Immunol.* **168,** 3697–3701
87. Mantovani, A., Sica, A., Sozzani, S., Allavena, P., Vecchi, A., and Locati, M. (2004) The chemokine system in diverse forms of macrophage activation and polarization. *Trends Immunol.* **25,** 677–686
88. Gordon, S. (2003) Alternative activation of macrophages. *Nat. Rev. Immunol.* **3,** 23–35
89. Murray, H. W., Spitalny, G. L., and Nathan, C. F. (1985) Activation of mouse peritoneal macrophages *in vitro* and *in vivo* by interferon-γ. *J. Immunol.* **134,** 1619–1622
90. Schroder, K., Hertzog, P. J., Ravasi, T., and Hume, D. A. (2004) Interferon-γ: an overview of signals, mechanisms and functions. *J. Leukoc. Biol.* **75,** 163–189
91. Taams, L. S., van Amelsfort, J. M., Tiemessen, M. M., Jacobs, K. M., de Jong, E. C., Akbar, A. N., Bijlsma, J. W., and Lafeber, F. P. (2005) Modulation of monocyte/macrophage function by human $CD4^+CD25^+$ regulatory T cells. *Hum. Immunol.* **66,** 222–230
92. Harding, C. V. (1995) Phagocytic processing of antigens for presentation by MHC molecules. *Trends Cell Biol.* **5,** 105–109
93. Blander, J. M., and Medzhitov, R. (2004) Regulation of phagosome maturation by signals from toll-like receptors. *Science* **304,** 1014–1018
94. Wang, Y., Chen, T., Han, C., He, D., Liu, H., An, H., Cai, Z., and Cao, X. (2007) Lysosome-associated small Rab GTPase Rab7b negatively regulates TLR4 signaling in macrophages by promoting lysosomal degradation of TLR4. *Blood* **110,** 962–971
95. Wang, Y. C., He, F., Feng, F., Liu, X. W., Dong, G. Y., Qin, H. Y., Hu, X. B., Zheng, M. H., Liang, L., Feng, L., Liang, Y. M., and Han, H. (2010) Notch signaling determines the M1 versus M2 polarization of macrophages in antitumor immune responses. *Cancer Res.* **70,** 4840–4849
96. Kim, R., Emi, M., and Tanabe, K. (2005) Cancer cell immune escape and tumor progression by exploitation of anti-inflammatory and pro-inflammatory responses. *Cancer Biol. Ther.* **4,** 924–933
97. Baecher-Allan, C., and Hafler, D. A. (2006) Human regulatory T cells and their role in autoimmune disease. *Immunol. Rev.* **212,** 203–216
98. Gereda, J. E., Leung, D. Y., Thatayatikom, A., Streib, J. E., Price, M. R., Klinnert, M. D., and Liu, A. H. (2000) Relation between house-dust endotoxin exposure, type 1 T-cell development, and allergen sensitisation in infants at high risk of asthma. *Lancet* **355,** 1680–1683